THE JOURNAL OF BIOLOGICAL CHEMISTRY
Vol. 272, No. 7, Issue of February 14, pp. 4582–4590, 1997

Printed in U.S.A.

A Structural Change Occurs upon Binding of Syntaxin to SNAP-25*

(Received for publication, September 8, 1996, and in revised form, November 13, 1996)

Dirk Fasshauer‡, Dieter Bruns§, Betty Shen¶, Reinhard Jahn‡§, and Axel T. Brünger§¶‖

From the §Howard Hughes Medical Institute and the ‡Department of Pharmacology, Yale University School of Medicine, and the ¶Department of Molecular Biochemistry and Biophysics, Yale University, New Haven, Connecticut 06510

The highly conserved proteins syntaxin and SNAP-25 are part of a protein complex that is thought to play a key role in exocytosis of synaptic vesicles. Previous work demonstrated that syntaxin and SNAP-25 bind to each other with high affinity and that their binding regions are predicted to form coiled coils. Circular dichroism spectroscopy was used here to study the α-helicity of the individual proteins and to gain insight into structural changes associated with complex formation. Syntaxin displayed approximately 43% α-helical content. In contrast, the α-helical content of SNAP-25 was low under physiological conditions. Formation of the SNAP-25-syntaxin complex was associated with a dramatic increase in α-helicity. Interaction of a 90-residue NH_2-terminal fragment of SNAP-25 comprising the minimal syntaxin binding domain lead to a similar but less pronounced increase in α-helicity. Single amino acid replacements in the putative hydrophobic core of this fragment with hydrophilic amino acids abolished the induced structural change and disrupted the interaction monitored by binding assays. Replacements with hydrophobic residues had no effect. Our findings are consistent with induced coiled coil formation upon binding of syntaxin and SNAP-25.

Neurotransmitters are released from presynaptic nerve endings by Ca^{2+}-triggered exocytosis of synaptic vesicles. Several lines of evidence suggest that exocytotic membrane fusion is mediated by a complex of conserved proteins which includes the synaptic vesicle protein synaptobrevin (also referred to as vesicle-associated membrane protein or VAMP) and the synaptic membrane proteins syntaxin and SNAP-25. Homologs of these neuronal proteins have been identified in many non-neuronal cell types including the yeast *Saccharomyces cerevisiae*, suggesting that the mechanism of exocytotic membrane fusion is conserved in all eukaryotic cells (for review, see Refs. 1–4).

Although the evidence linking these proteins to membrane fusion is quite compelling, very little is known about their mechanism of action. Rothman and colleagues (5) found that the three membrane proteins form a complex that interacts with additional soluble proteins known to support membrane fusion in cell-free extracts (5). These soluble proteins include the SNAPs[1] (soluble NSF attachment proteins) with three isoforms (α-, β- (brain-specific), and γ-SNAP), and the ATPase NSF (*N*-ethylmaleimide-sensitive fusion protein). SNAPs and NSF apparently operate on all relatives of the synaptobrevin/syntaxin/SNAP-25 protein families, which are therefore commonly referred to as SNAREs (SNAP receptors). ATP hydrolysis by NSF leads to disassembly of the synaptobrevin-syntaxin-SNAP-25-complex (6), an effect that is associated with a different state of syntaxin (7, 8).

Ultimately, vesicle docking and membrane fusion can be viewed as a series of sequential protein assembly and disassembly steps which may involve structural changes and regulated interactions of at least some of the proteins with the participating phospholipid bilayers. It is therefore of interest to understand the structural basis of these processes.

The three proteins synaptobrevin, syntaxin, and SNAP-25 assemble spontaneously into a complex that sediments at 7 S (5) and which is resistant to mild treatment by SDS (9, 10). A complex with very similar properties can be assembled *in vitro* from recombinant proteins that lack their transmembrane domains (syntaxin, synaptobrevin) or lack their posttranslationally added palmitoyl side chains (SNAP-25), respectively. The *in vitro* complex is also resistant to mild SDS treatment and can be disassembled by NSF in the presence of ATP (9). Each of these three proteins can bind to one of its two partners, forming binary complexes. SNAP-25 binds syntaxin with high affinity (EC_{50} of about 0.4 μM for SNAP-25) (11), whereas the binding affinity between syntaxin and synaptobrevin is weakest (12).

Truncation-, deletion-, and site-directed mutagenesis have revealed the minimal essential domains of each of the proteins which participates in the formation of the binary and the ternary complexes (9, 12–14). For the interaction between SNAP-25 and syntaxin, the NH_2-terminal half of SNAP-25 (amino acids 2–82 of SNAP-25) and the COOH-terminal domain of syntaxin (amino acids 199–243, also referred to as the H3 domain (14)) are required (9, 13). The H3 domain of syntaxin is also sufficient to bind synaptobrevin (12, 14). Interestingly, the interaction of SNAP-25 with synaptobrevin requires both the NH_2- and COOH-terminal domain of the SNAP-25 molecule (13). The binding of synaptobrevin to either syntaxin or SNAP-25 requires most of the conserved part of synaptobrevin (amino acids 27–96, excluding the transmembrane region) (9).

We have used circular dichroism (CD) spectroscopy to study the secondary structure of syntaxin and SNAP-25 and that of their binary complex. Although CD spectroscopy is incapable of providing detailed structural information it can be used to assess the approximate α-helical content of a protein. Furthermore, it can be used to assess changes of secondary structure which occur upon modification of the environment or upon complex formation. The SNAP-25 and syntaxin variants from

* This work was supported by a grant from the Deutsche Forschungsgemeinschaft (to D. F.) and by National Institutes of Health Grant GM54160-01 (to A. T. B.). The costs of publication of this article were defrayed in part by the payment of page charges. This article must therefore be hereby marked "*advertisement*" in accordance with 18 U.S.C. Section 1734 solely to indicate this fact.

‖ To whom correspondence should be sent: Dept. Molecular Biophysics and Biochemistry, Bass Center, 266 Whitney Ave., New Haven, CT 06520. Tel.: 203-432-6143; Fax: 203-432-6946; E-mail: brunger@laplace.csb.yale.edu.

[1] The abbreviations used are: SNAP(s), soluble NSF attachment protein(s); NSF, *N*-ethylmaleimide-sensitive fusion protein; SNAP-25, synaptosomal associated protein of 25 kDa; SNARE, SNAP receptor; DTT, dithiothreitol; GST, glutathione *S*-transferase.

the leech (*Hirudo medicinalis*) were used in this study. Both are highly homologous to their mammalian counterparts.

EXPERIMENTAL PROCEDURES

Molecular Cloning of SNAP-25 and Syntaxin from Hirudo medicinalis—As part of our efforts to develop the Retzius cell of the leech (*H. medicinalis*) as a model system for studying the mechanisms of synaptic transmission (15), all experiments were based on leech syntaxin and leech SNAP-25 isoforms. cDNA clones encoding *H. medicinalis* syntaxin and SNAP-25 were isolated from a λ-Zap library prepared from the nerve cord of the leech. The leech variants of the synaptic proteins SNAP-25 and syntaxin exhibit high homology to their mammalian counterparts. A detailed description of the cloning strategy and the nucleotide sequences will be published elsewhere.[2] For the bacterial expression of recombinant proteins, full-length and truncated coding sequences were amplified using the polymerase chain reaction with oligonucleotides containing *Bam*HI and *Eco*RI restriction sites and subcloned into pGEX4-T (Pharmacia) or pTrcHisA (Invitrogen).

For the generation of full-length SNAP-25 (1–212) the sense and antisense primers were 5′-CCGGGATCCATGGCCAAGGATATCAAG-3 and 5′-GCGGAATTCTTATTCTTTCAGGAGTTTGC-3′, respectively. For the generation of the 3′ deletion mutant SNAP-$25_{1–90wt}$ the primer 5′-GCGGAATTCTTATTCCATCCCTTCCAGGTT-3′ was used. For the generation of the 5′ deletion mutant SNAP-$25_{112–212}$ the primer 5′-GCGGGATCCTGGAACAAGGGCGACGAGGGA-3′ was used. Leech syntaxin (residues 1–271, comprising the entire cytoplasmic domain) was constructed using primers that were complementary to codons of amino acids 1–6 and 266–271. Site-directed mutagenesis of SNAP-$25_{1–90}$ (see Fig. 8) was performed using the overlapping primer method (16). All mutants were confirmed by resequencing the entire coding region.

Purification of Recombinant Proteins—GST fusion proteins were purified by affinity chromatography on glutathione-Sepharose beads essentially as described (13) except that 20 mM Tris, pH 7.4, 150 mM NaCl, 1 mM EDTA, 1 mM DTT was used as chromatography buffer. Fusion proteins containing His_6 tags (expressed in pTrcHisA) were purified by Ni^{2+}-Sepharose chromatography as described (13). Proteins were eluted by increasing the imidazole concentration stepwise to 40, 80, 120, or 240 mM (in 20 mM Tris, pH 7.4, 500 mM NaCl). Fractions were analyzed for purity by SDS-polyacrylamide gel electrophoresis (17) and staining with Coomassie Blue. Imidazole-containing fractions with recombinant protein were dialyzed against FPLC-buffer A (10 mM Tris, pH 7.4, 100 mM NaCl, 1 mM EDTA, 1 mM DTT). His_6-tagged proteins were purified further by anion exchange chromatography on a Mono Q column using an FPLC system (Pharmacia Biotech Inc.). After loading, the proteins were eluted with a linear gradient from 100 to 1,000 mM NaCl, and fractions containing the purified proteins were pooled. For the purification of the binary complex of SNAP-25 and syntaxin, both purified proteins were incubated overnight, dialyzed against FPLC-buffer A, loaded on a Mono Q column, and eluted with a linear gradient from 100 to 1,000 mM NaCl. The peak fractions were pooled, and its homogeneity was verified by size exclusion chromatography on an HR-10/30 Superdex 200 column (Pharmacia).

CD Spectroscopy—Far UV-CD spectra were obtained by averaging 5–20 scans with a step size of 0.5 nm on an AVIV model 62DS CD spectrometer at 25 °C. All measurements were performed in a Hellma quartz cuvette with a path length of 0.1 or 0.5 cm. All CD spectra were performed with purified His_6-tagged proteins (pTrcHisA). After purification the proteins were dialyzed against 10 mM phosphate buffer, pH 7.4, containing 100 mM NaCl (standard conditions) and concentrated by ultrafiltration to final concentrations of 1–10 mg/ml. Protein concentrations of SNAP-$25_{1–90}$ fragments and of the purified SNAP-25-syntaxin complex were calibrated by internally standardized amino acid analysis following acid hydrolysis (carried out by the W. M. Keck Foundation Biotechnology Resource Laboratory at Yale University) and subsequentially determined by measuring absorbance at 280 nm. Protein concentrations of SNAP-$25_{112–212}$-fragment, $syntaxin_{1–271}$, and full-length SNAP-25 were determined by the Coomassie Blue binding method (18). Unless indicated otherwise, all recordings for single proteins were performed in 10 mM sodium phosphate buffer, pH 7.4, 100 mM NaCl.

The CD spectra of SNAP-25-syntaxin complexes were recorded after reaching equilibrium following an overnight incubation at 4 °C in 10 mM phosphate buffer, pH 7.4, 100 mM NaCl, 2 mM $MgCl_2$, 1 mM EDTA, 1 mM DTT, comparable to the conditions used for binding assays with GST fusion proteins. To evaluate changes of the CD spectrum attributable to complex formation, the theoretical noninteracting spectrum was calculated from the spectra of the individual proteins using the equation $[\Theta]_{sum} = (c_1n_1[\Theta]_1 + c_2n_2[\Theta]_2)/(c_1n_1 + c_2n_2)$, where c_1 and c_2 are the respective concentrations of peptide molarity, n_1 and n_2 are respective number of amino acids, and $[\Theta]_1$ and $[\Theta]_2$ are the observed mean residue ellipticities of the two proteins. The CD spectrum of the purified SNAP-25-syntaxin complex was recorded in 10 mM Tris, pH 7.4, 300 mM NaCl, 1 mM EDTA, 1 mM DTT. The molar ellipticity was calculated assuming a 1:1 complex.

The fractional α-helical content for each protein was calculated using the assumption that for 100% α-helix the mean residue ellipticity, [Θ], at 222 nm is $[\Theta]_{222} = -36{,}300\ (1–2.57/X)$, where X is the number of amino acids in the protein (19).

Size Exclusion Chromatography—Size exclusion chromatography was performed on an HR-10/30 Superdex 200 column (Pharmacia) in 10 mM sodium phosphate buffer, pH 7.4, containing NaCl concentrations as indicated at a flow rate of 0.5 ml/min at 25 °C. The elution profiles were monitored photometrically at 280 nm. 200 μl of protein solution (10 μM of protein) was loaded. Globular proteins that were used as molecular mass standards were loaded at a concentration of 1.0 mg/ml and included alcohol dehydrogenase, bovine serum albumin, ovalbumin, carbonic anhydrase, and myoglobulin (molecular mass = 150, 66, 45, 29.5, and 17 kDa, respectively).

Binding to Glutathione-Sepharose-immobilized Proteins—Soluble proteins were incubated together with indicated amounts of GST fusion protein immobilized on glutathione-Sepharose beads in binding buffer (20 mM Tris, pH 7.4, 150 mM NaCl, 1 mM EDTA, 2 mM $MgCl_2$, 1 mM DTT). Incubations were carried out overnight at 4 °C. The beads were then washed three times in 1 ml of binding buffer. Proteins bound to the beads were finally solubilized in SDS sample buffer (final concentrations: 60 mM Tris, pH 6.8, 2% SDS, 10% glycerine, 3% β-mercaptoethanol) and heated for 5 min at 95 °C, subjected to SDS-polyacrylamide gel electrophoresis and immunoblot analysis using T7-tagged monoclonal antibody (Novagen). The blots were stained with an alkaline phosphatase-conjugated secondary antibody using nitro blue tetrazolinum and 5-bromo-4-chloro-3-indolyl phosphate.

Prediction of Coiled Coils—For the prediction of coiled coil domains the Lupas (20, 21) and the paircoil algorithm (22) were used. The programs were accessed through the Internet.[3] ulrec3.unil.ch/software/COILS_form.html and http://ostrich.lcs.mit.edu/cgi-bin/score).

RESULTS

CD Spectroscopy of Syntaxin and SNAP-25—CD spectra of SNAP-25 and syntaxin are shown in Fig. 1*A* in 10 mM phosphate buffer and 100 mM NaCl, pH 7.4. The CD spectrum of syntaxin, with two clearly defined minima at 208 and 222 nm, suggests an α-helical content of approximately 43%. In contrast, the CD spectrum of SNAP-25 indicates little α-helical content (approximately 14%) and is reminiscent of partially unstructured proteins (23).

For more detailed studies of the interaction between SNAP-25 and syntaxin, a NH_2-terminal fragment of SNAP-25 was generated which comprises the minimal domain required for syntaxin binding (SNAP-$25_{1–90wt}$). This fragment showed a slightly higher α-helical content (approximately 20%) than the full-length protein (Fig. 1*B*). The CD spectrum of SNAP-$25_{1–90wt}$ did not change when the protein concentration was varied more than 100-fold (ranging from 0.3 to 36 mM, Fig. 1*C*). A fragment of the COOH-terminal half of SNAP-25 (SNAP-$25_{112–212}$) exhibited a CD spectrum similar to that of the full-length protein, with an α-helical content of approximately 13% (Fig. 1*B*).

Increasing NaCl concentrations lead to a dramatic increase [1]of the α-helicity of SNAP-$25_{1–90wt}$ (Fig. 2, *A* and *B*), with minima at 208 and 222 nm clearly visible already at a concentration of 300 mM NaCl. The α-helical content in 1 M NaCl was about 44%. To investigate if the increased α-helical content at higher ionic strength was associated with a change in the

[2] Bruns, D., Engers, S., Yang, C., Ossig, R., Jeromin, A., and Jahn, R. (1997) *J. Neurosci.*, in press.

[3] Programs are available on the World Wide Web (URLs: http://ulrec3.unil.ch/software/COILS_form.html and http://ostrich.lcs.mit.edu/cgi-bin/score).

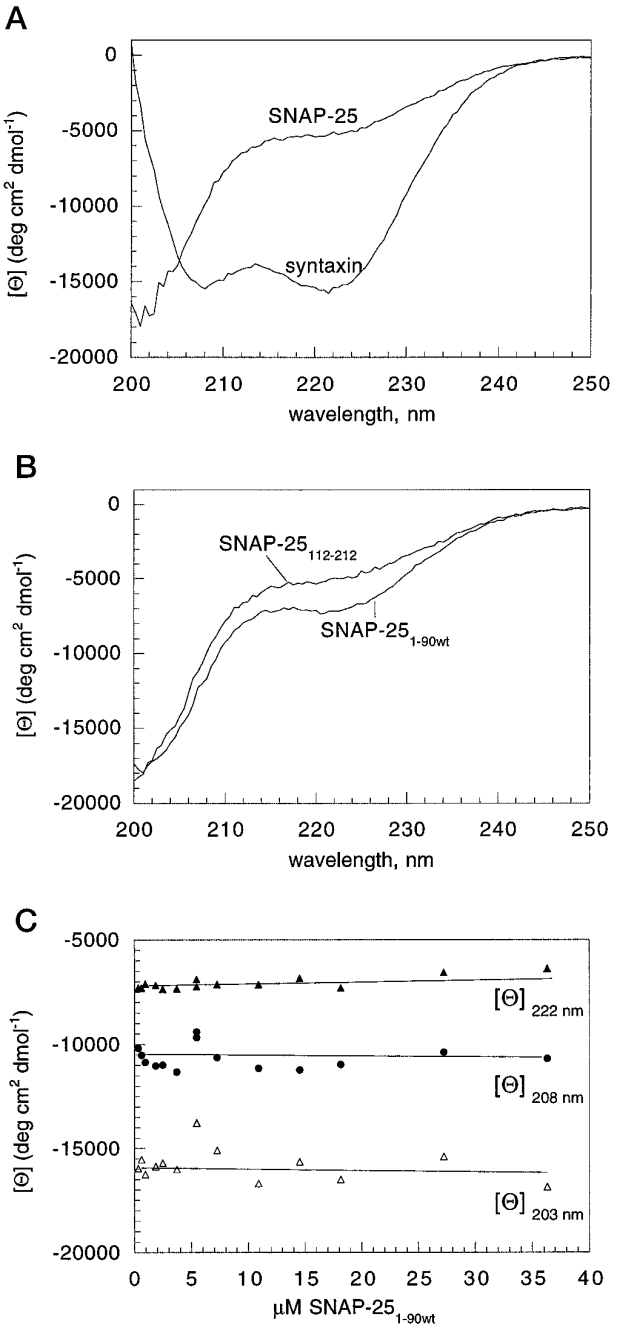

FIG. 1. **CD spectra of syntaxin, SNAP-25, and SNAP-25 fragments at standard conditions.** *Panel A*, CD spectra of full-length SNAP-25 and syntaxin$_{1-271}$. *Panel B*, CD spectra of SNAP-25$_{1-90wt}$ and SNAP-25$_{112-212}$. *Panel C*, mean residue ellipticity ([Θ]) at 222, 208, and 203 nm for different concentrations of SNAP-25$_{1-90wt}$.

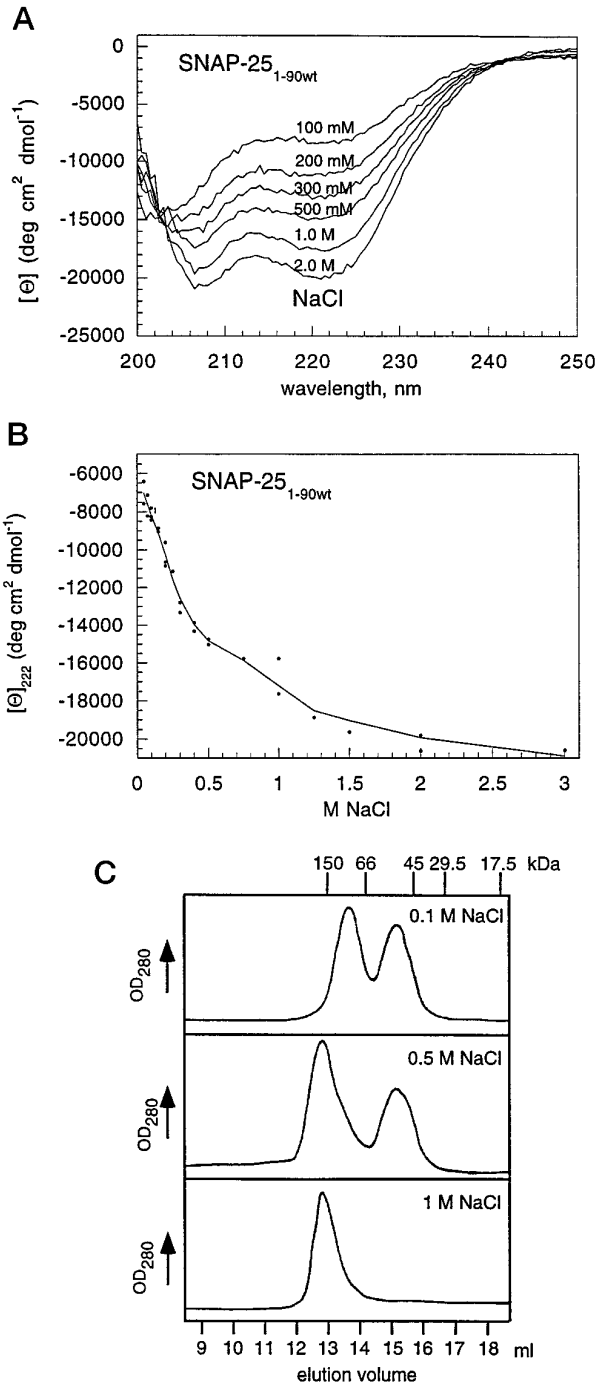

FIG. 2. **Increase of α-helicity and change of the oligomeric state of SNAP-25$_{1-90wt}$ by increasing concentrations of NaCl.** In the experiments standard conditions were used except that NaCl concentrations were adjusted as indicated. *Panel A*, effect of increasing NaCl concentrations on the CD spectra of SNAP-25$_{1-90wt}$. *Panel B*, the mean residue ellipticity ([Θ]) at 222 nm of SNAP-25$_{1-90wt}$ spectra is plotted against NaCl concentrations. *Panel C*, size exclusion chromatography of SNAP-25$_{1-90wt}$ at different NaCl concentrations. A Superdex-200 column was loaded with 200 μl of SNAP-25$_{1-90wt}$ (approximately 10 μM) at 25 °C in 10 mM sodium phosphate buffer at the NaCl concentrations indicated and eluted with the same buffer. Column effluent was monitored at an OD of 280 nm. *Arrows* indicate the positions of globular proteins used as molecular mass standards (see "Experimental Procedures").

oligomeric state of the molecule, samples were analyzed by size exclusion chromatography. In 100 mM NaCl, SNAP-25$_{1-90wt}$ eluted in two peaks with apparent molecular masses of 50 and 90 kDa. At 500 mM NaCl the molecule eluted in two peaks with apparent molecular masses of 50 and 160 kDa. When the NaCl concentration was raised to 1 M, the protein eluted as a single peak of molecular mass of 160 kDa (Fig. 2*C*). Apparently, high ionic strength induced the formation of a defined higher order oligomer with apparent molecular mass of 160 kDa, whereas in low salt the protein structure is undefined, and the two peaks may correspond to different oligomeric species. The view that SNAP-25$_{1-90wt}$ is more structured in high salt was further supported by limited tryptic digestion of the protein. In high salt, only partial digestion was observed, resulting in a defined fragment of reduced size, whereas in 100 mM NaCl the protein was digested into small fragments (not shown).

Divalent cations were about 100-fold more potent than

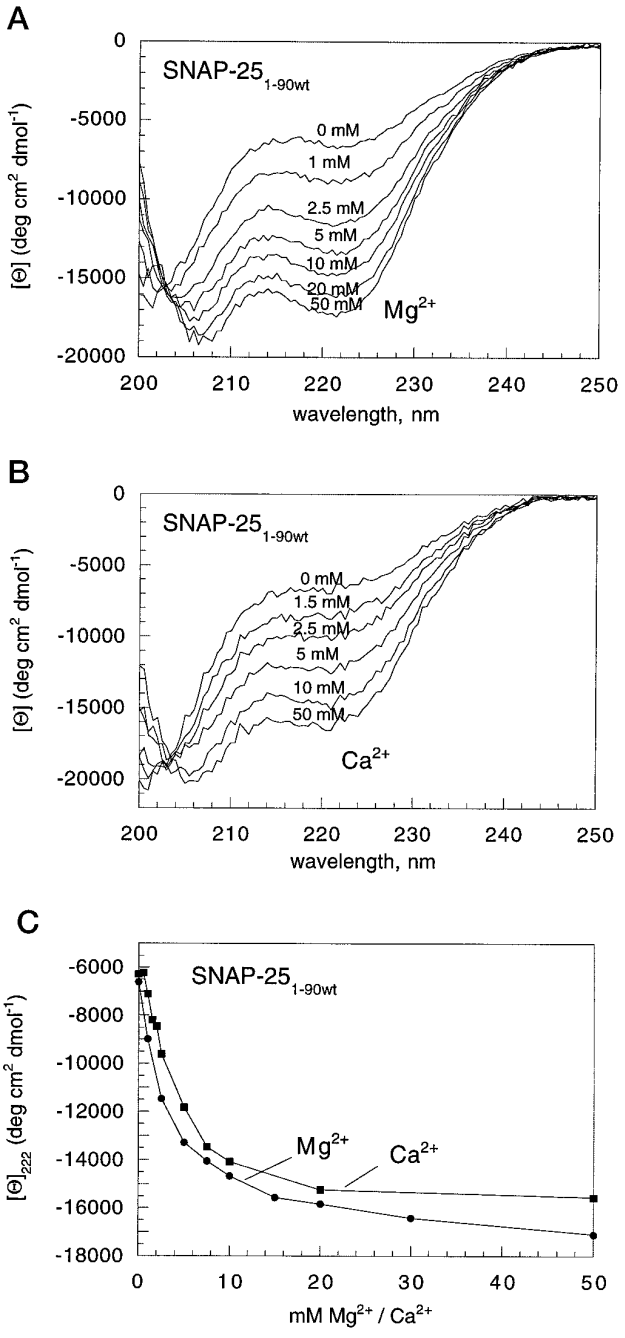

FIG. 3. **Increase of α-helicity of SNAP-25$_{1–90wt}$ induced by increasing concentrations of divalent cations.** All recordings were done under standard conditions supplemented as indicated. When $CaCl_2$ was added the phosphate buffer was replaced with 10 mM Tris-Cl, pH 7.4. *Panel A*, effect of $MgCl_2$ concentration on the CD spectra of SNAP-25$_{1–90wt}$. *Panel B*, effect of $CaCl_2$ concentration on the CD spectra of SNAP-25$_{1–90wt}$. *Panel C*, the mean residue ellipticity ([Θ]) at 222 nm of SNAP-25$_{1–90wt}$ spectra is plotted against $MgCl_2$ and $CaCl_2$ concentrations.

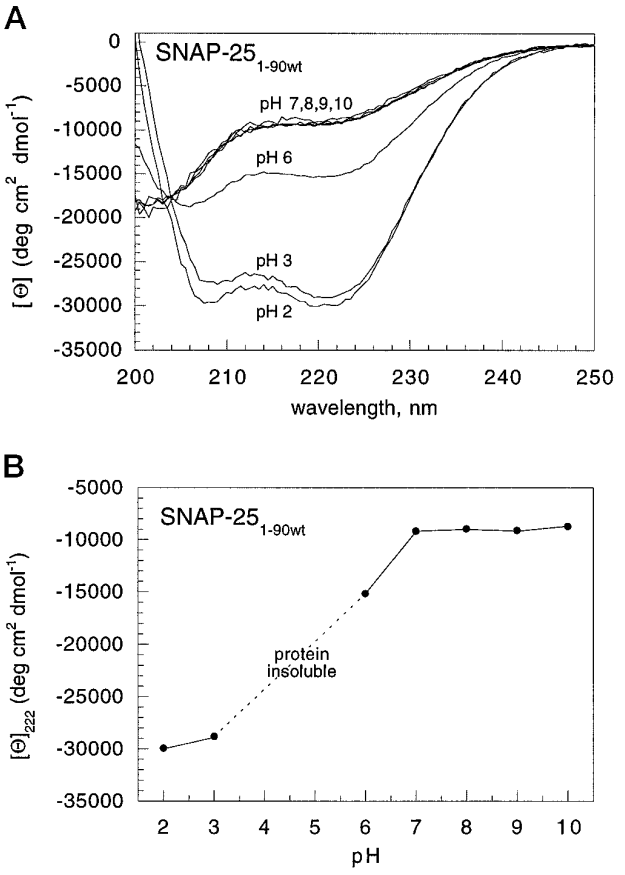

FIG. 4. **Changes in the CD spectra of SNAP-25$_{1–90wt}$ caused by variations of the pH.** Recordings were obtained in 100 mM sodium phosphate, pH-adjusted with NaOH, containing 100 mM NaCl. *Panel A*, effect of pH on the CD spectra of SNAP-25$_{1–90wt}$. *Panel B*, the mean residue ellipticity ([Θ]) at 222 nm of SNAP-25$_{1–90wt}$ spectra is plotted against pH.

monovalent cations in inducing α-helical structure in SNAP-25$_{1–90wt}$ (Fig. 3) with both Mg^{2+} and Ca^{2+} being effective. This potency is only partially attributable to the increased ionic strength because similar concentrations of divalent anions were ineffective (not shown). Rather, it may be due to more efficient shielding of charges or formation of salt bridges between negatively charged residues.

As shown in Fig. 4, lowering the pH to 6.0 also increased the α-helical content in SNAP-25$_{1–90wt}$. At pH 3 the α-helical content increased even further. This may be explained by the fact that SNAP-25$_{1–90wt}$ is negatively charged at neutral pH (calculated pI = 4.55 including the His_6 tag; note also that the protein was insoluble at pH values around its isoelectric point). Negatively charged groups become protonated at low pH, thus neutralizing potential charge-charge repulsions (24).

As mentioned above, the α-helical content of full-length SNAP-25 was somewhat lower than that of the NH_2-terminal fragment SNAP-25$_{1–90}$. The increase in its α-helical content in high salt or at low pH was also less pronounced (19% in 1 M NaCl; 38% at pH 3) than for the NH_2-terminal fragment. When the COOH-terminal fragment of SNAP-25 (SNAP-25$_{112–212}$) was analyzed at high ionic strength or at low pH, no increase in α-helical content was observed (not shown). This suggests that the α-helical structure induced by these environmental changes is confined to the NH_2-terminal half of the molecule.

Structural Changes Induced by Complex Formation—In the next series of experiments we investigated whether the binding of SNAP-25 to syntaxin was associated with changes in secondary structure. For this purpose, CD spectra were obtained after an overnight incubation of approximately equimolar concentrations of syntaxin and full-length SNAP-25. The CD spectrum of this complex was compared with the sum of spectra (*i.e.* theoretical, noninteracting) that were recorded for each individual protein, corrected for variations of the protein concentrations (see "Experimental Procedures").

As shown in Fig. 5*A*, the CD spectrum of the SNAP-25-syntaxin complex was clearly more α-helical than the theoretical noninteracting sum of the individual spectra, demonstrating that the complex had a higher α-helical content than the

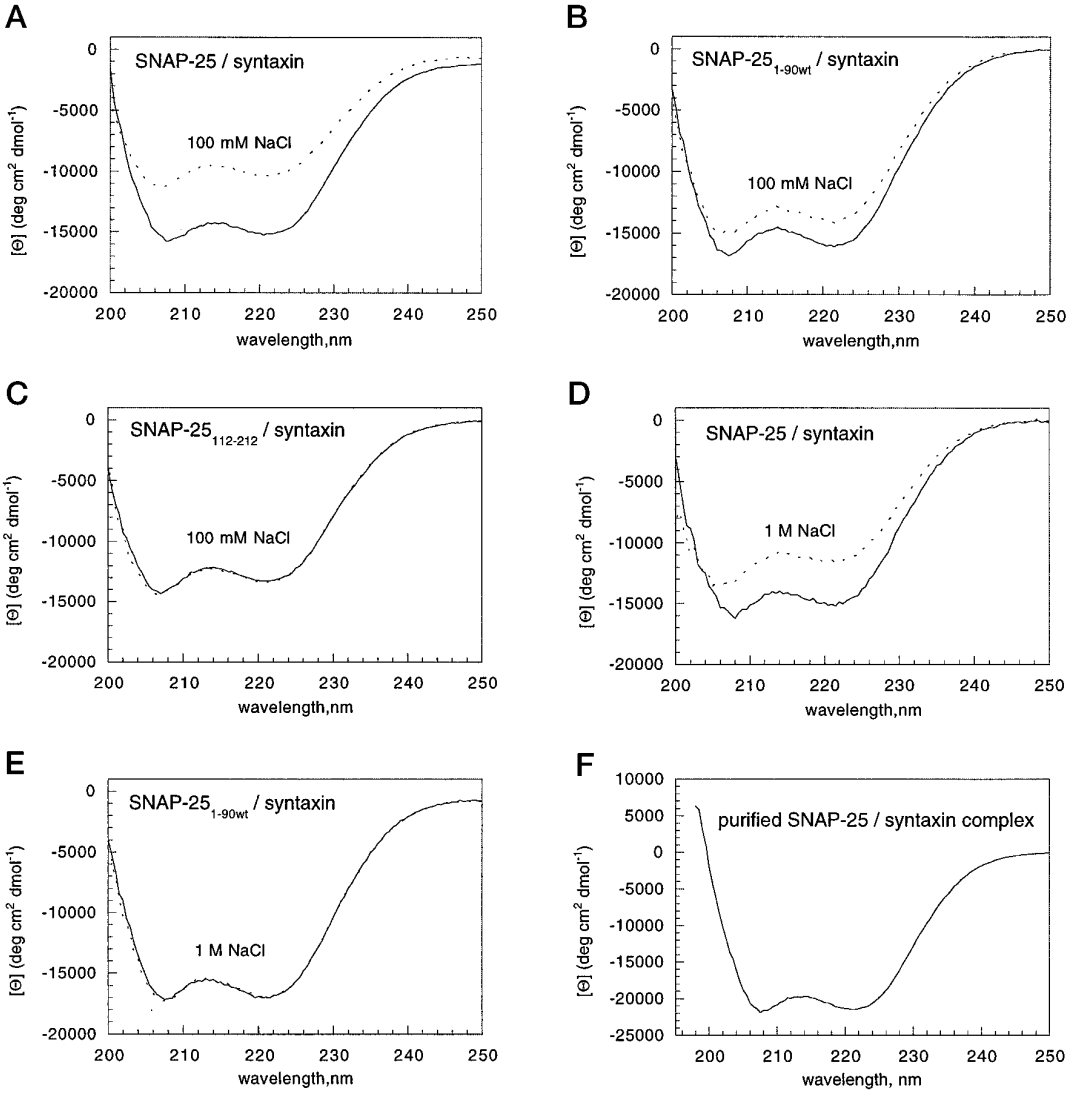

FIG. 5. **Changes in the CD spectra caused by interaction between SNAP-25 and syntaxin.** If not indicated otherwise, CD spectra were recorded in 10 mM sodium phosphate, pH 7.4, 2 mM $MgCl_2$, 1 mM EGTA, 1 mM DTT, with the NaCl concentrations indicated in the *panels*. Spectra of each individual binding partner were recorded, and the sum of both spectra was calculated (*dotted line*; corrected for variations of the protein concentrations; for details, see "Experimental Procedures"). The spectra of the combined components (*solid line*) were recorded after overnight incubation of the binding partners. *Panel A*, full-length SNAP-25 (8.7 μM) plus syntaxin$_{1-271}$ (7.1 μM) in 100 mM NaCl. *Panel B*, SNAP-25$_{1-90wt}$ (6.2 μM) plus syntaxin$_{1-271}$ (7.1 μM) in 100 mM NaCl. *Panel C*, SNAP-25$_{112-212}$ (9.8 μM) plus syntaxin$_{1-271}$ (16.4 μM) in 100 mM NaCl. *Panel D*, full-length SNAP-25 (2.9 μM) plus syntaxin$_{1-271}$ (2.7 μM) in 1 M NaCl. *Panel E*, SNAP-25$_{1-90wt}$ (3.1 μM) plus syntaxin$_{1-271}$ (2.7 μM) in 1 M NaCl. *Panel F*, CD spectrum of the purified SNAP-25-syntaxin complex. Purification consisted of anion exchange chromatography. The spectrum was recorded in 300 mM NaCl, 10 mM Tris-HCl, pH 7.4, 1 mM EDTA, 1 mM DTT at 25 °C.

individual components alone. A similar but less pronounced increase was observed when the NH_2-terminal fragment of SNAP-25 (SNAP-25$_{1-90wt}$) instead of the full-length protein (Fig. 5*B*) was used in the binding reaction. In contrast, no increase in α-helicity was observed upon mixing of the COOH-terminal half of SNAP-25 (SNAP-25$_{112-212}$) with syntaxin (Fig. 5*C*).

The observed increase in α-helicity during complex formation may be due to a change in SNAP-25 alone, in syntaxin alone, or in both proteins. However, the CD spectrum of syntaxin did not change under any of the environmental conditions tested (high salt, divalent ions, high or low pH; not shown), whereas α-helicity could readily be induced in SNAP-25. This suggests that the increase in α-helicity upon complex formation is due to a change in SNAP-25.

CD spectra of the complexes were also recorded in high salt (1 M NaCl; Fig. 5, *D* and *E*). When the spectra were compared with the theoretical noninteracting sum of the spectra of the individual components under these conditions, the induced α-helicity was less pronounced in the SNAP-25-syntaxin complex, and no induction was observed in the SNAP-25$_{1-90wt}$-syntaxin complex. Since the induced α-helicity was always larger for the full-length SNAP-25-syntaxin complex than for the SNAP-25$_{1-90wt}$-syntaxin complex, it is likely that the COOH-terminal half of SNAP-25 also becomes more structured upon complex formation.

Although binding experiments have demonstrated that binding of full-length SNAP-25 to syntaxin occurs with high affinity, it cannot be excluded that dynamic equilibria exist which may contribute to the spectrum. For these reasons, the binary complex was purified by ion exchange chromatography, and its homogeneity was verified by size exclusion chromatography. No measurable dissociation occurred during purification (data not shown). The purified complex has a CD spectrum that is very similar to that of the complex formed directly from its constituents without further purification (compare Fig. 5, *F*

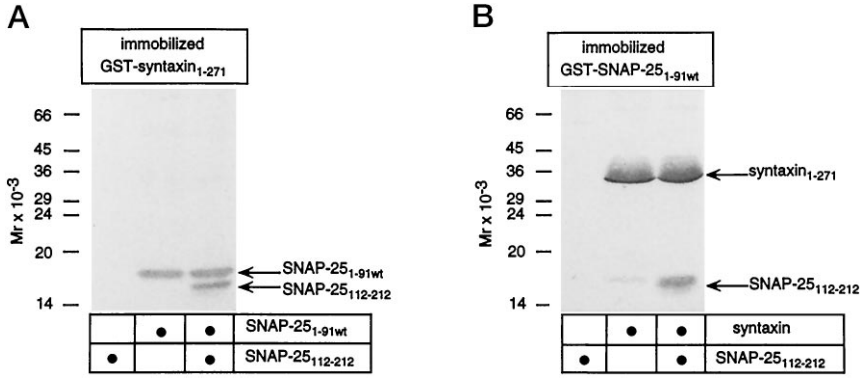

FIG. 6. **Binding of the COOH-terminal half of SNAP-25 to a complex of SNAP-25$_{1–90wt}$ and syntaxin.** *Panel A*, 10 μg of GST-syntaxin$_{1–271}$ immobilized on glutathione-Sepharose was incubated overnight at 4 °C with 500 μl of the indicated His$_6$-tagged fragments of SNAP-25 (each about 10 μM). *Panel B*, 10 μg of GST-SNAP-25$_{1–90wt}$ immobilized on glutathione-Sepharose was incubated overnight at 4 °C with 500 μl the His$_6$-tagged proteins as indicated (each about 10 μM). Proteins bound to the beads were analyzed by an immunoblot assay using the monoclonal T7-tagged antibody against a recognition domain in the His$_6$-tag (TrcHisA). The NH$_2$-terminal half of SNAP-25 binds to syntaxin, whereas the COOH-terminal half of SNAP-25 only binds to a complex of the NH$_2$-terminal half of SNAP-25 and syntaxin.

and *D*), although the molar ellipticities are somewhat higher. This indicates that in the mixing experiments the resulting CD spectrum is determined mainly by the complex.

No direct binding of a COOH-terminal fragment of SNAP-25 to syntaxin has been described in previous studies (9, 13). This suggests that the COOH-terminal fragment of SNAP-25 might bind only when a complex between syntaxin and the NH$_2$-terminal fragment of SNAP-25 has formed. To confirm this idea, GST-syntaxin, immobilized on glutathione-Sepharose, was incubated sequentially with SNAP-25$_{1–90wt}$ and SNAP-25$_{112–212}$. As shown in Fig. 6*A*, SNAP-25$_{112–212}$ bound to syntaxin when SNAP-25$_{1–90wt}$ was present, whereas no binding was observed to syntaxin alone. A similar result was obtained when GST-SNAP-25$_{1–90wt}$ was immobilized. Again, binding of SNAP-25$_{112–212}$ was dependent on the presence of syntaxin (Fig. 6*B*).

Effect of Single Amino Acid Substitutions of SNAP-25—In the last series of experiments, amino acid substitutions were introduced in the NH$_2$-terminal fragment of SNAP-25 to investigate how changes in the ability to bind syntaxin correlate with structural changes observed by CD. The first mutation consisted of a glycine to aspartic acid substitution in the highly conserved (*cf.* Fig. 8) position 51 (SNAP-25$_{1–90GD}$). This substitution was motivated by a similar exchange at the homologous position in the yeast Sec9-protein which results in a temperature-dependent loss of function phenotype (25). *Sec9* is an essential gene in yeast which is required for the final exocytotic step in the constitutive membrane trafficking pathway. Although Sec9p is considerably larger than SNAP-25, the COOH-terminal domain, which is homologous to SNAP-25, is apparently sufficient to sustain wild type function (25), suggesting that Sec9 is a member of the SNAP-25 protein family. As shown in Fig. 7*A*, the SNAP-25$_{1–90GD}$ variant was unable to bind to syntaxin.

In the second set of mutations, either one or both of two conserved hydrophobic amino acids, Met-40 and Met-43, were replaced with glutamate residues (SNAP-25$_{1–90M40E}$, SNAP-25$_{1–90M43E}$, and SNAP-25$_{1–90EE}$). No binding of these mutants to GST-syntaxin was observed (Fig. 7*A*). In parallel, we substituted both methionines with leucines (SNAP-25$_{1–90LL}$), *i.e.* a hydrophobic but structurally different amino acid with a comparable side chain volume. In fact, several SNAP-25 variants contain leucine at position 43, whereas Met-40 is conserved (see Fig. 8). As shown in Fig. 7*A*, the resultant mutant protein bound to syntaxin in a manner indistinguishable from wild type.

The CD spectra of the mutant proteins had a shape similar to that of SNAP-25$_{1–90wt}$, but they differed in their α-helical content (Fig. 7*B*). SNAP-25$_{1–90LL}$ showed higher α-helicity than wild type, whereas SNAP-25$_{1–90EE}$ had lower α-helicity (Fig. 7*B*), an effect that was less pronounced for the single site mutants SNAP-25$_{1–90M40E}$ and SNAP-25$_{1–90M43E}$ (not shown). Similarly, substitution of Gly-51 with aspartic acid (SNAP-25$_{1–90GD}$) reduced the α-helical content (Fig. 7*B*). These differences between the α-helical contents of the binding and nonbinding mutants became more pronounced at high ionic strength or in the presence of divalent cations (not shown). All SNAP-25$_{1–90}$ variants had a high α-helical content at pH 3. Apparently, protonation of the glutamate (SNAP-25$_{1–90EE}$) or the aspartate side chains (SNAP-25$_{1–90GD}$) restores the ability of these mutants to form α-helices.

Upon interaction with syntaxin the binding mutant SNAP-25$_{1–90LL}$ exhibited an increase in α-helicity which was very similar to that of the wild type fragment (Fig. 7*C*). In contrast, no difference between the measured and calculated CD spectra was observed when the nonbinding mutants (SNAP-25$_{1–90EE}$ and SNAP-25$_{1–90GD}$) were mixed with syntaxin (Fig. 7, *D* and *E*).

DISCUSSION

The binding of syntaxin and SNAP-25 is thought to be part of a sequence of protein-protein interactions that leads from vesicle docking to membrane fusion. Although an increasing number of these interactions are known and the participating protein domains have been identified, no biophysical and structural information regarding these interactions has been available up to now. The CD data presented here demonstrate that the formation of a binary complex between syntaxin and SNAP-25 is associated with a dramatic increase in α-helical content which presumably occurs mainly in SNAP-25.

Is the interaction between the two proteins mediated by direct interaction between adjacent α-helices? Several investigators noted earlier that the minimal binding domains of both SNAP-25 and syntaxin have a high propensity for the formation of coiled coils (9, 13, 14, 25) and suggested that binding is mediated by such interactions. The dramatic increase in α-helical content upon complex formation is consistent with an induced coiled coil formation, although alternative structures cannot be excluded at present. Two-stranded coiled coils consist of two amphipathic right-handed α-helices that are twisted around each other, forming a left-handed superhelix (26). The individual helices bury hydrophobic residues along one side of the helix. These side chains form the hydrophobic core of the superhelix and are often flanked by charged side chains that

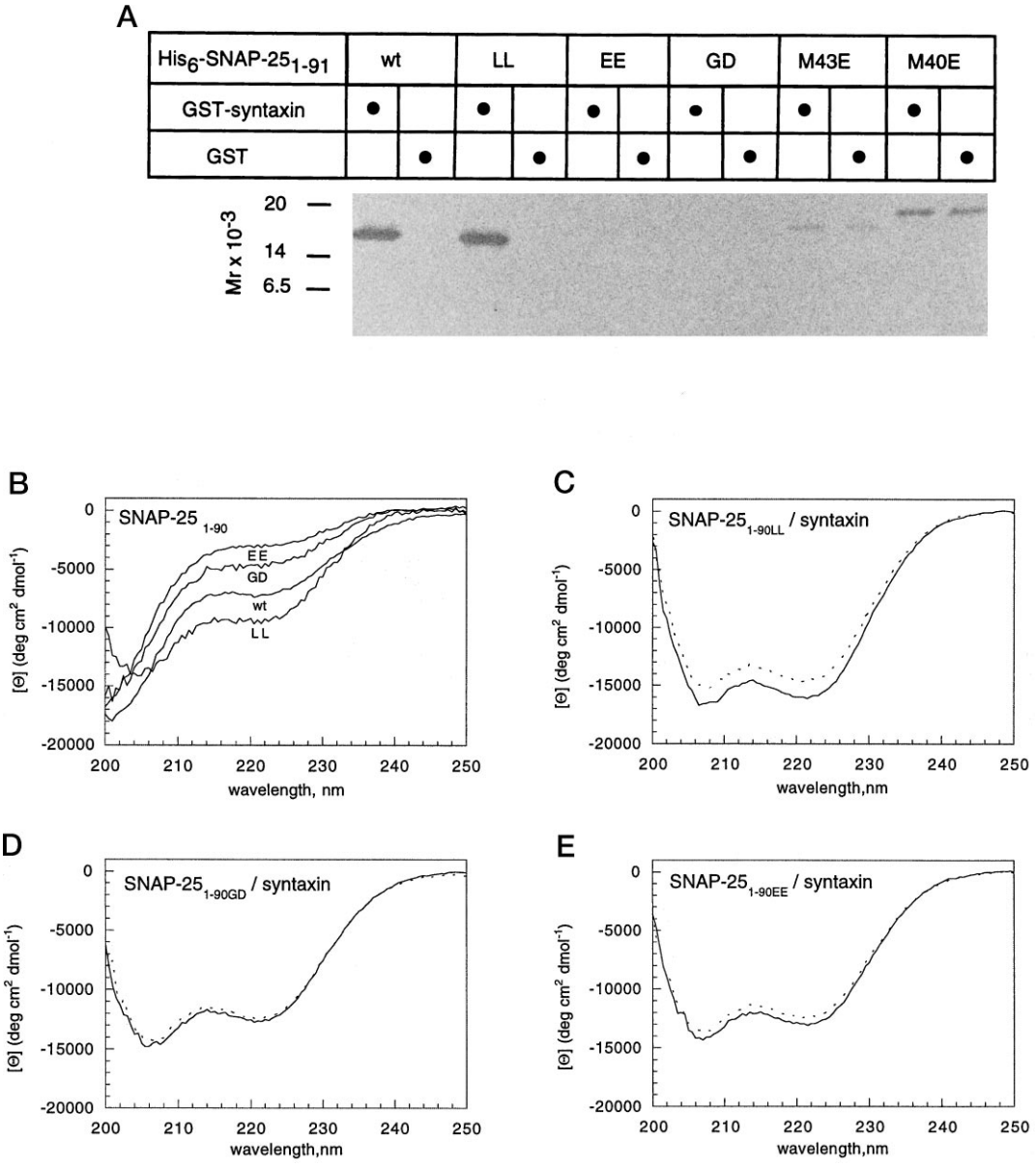

FIG. 7. **Mutants of SNAP-25$_{1–90}$: CD spectroscopy and binding properties.** *Panel A*, binding of SNAP-25$_{1–90}$ fragments to GST-syntaxin$_{1–271}$ or GST, immobilized on glutathione beads. The figure shows protein retained on the beads, analyzed by immunoblotting (see Fig. 7 for details). SNAP-25$_{1–90wt}$ and SNAP-25$_{1–90LL}$ bind specifically to GST-syntaxin$_{1–271}$, whereas the mutants SNAP-25$_{1–90GD}$, SNAP-25$_{1–90EE}$, SNAP-25$_{1–90M40E}$, and SNAP-25$_{1–90M43E}$ do not bind to syntaxin. The mutants SNAP-25$_{1–90M40E}$ and SNAP-25$_{1–90M43E}$ exhibit only nonspecific binding to syntaxin. *Panel B*, CD spectra of mutated SNAP-25$_{1–90}$ fragments in standard conditions. *Panels C–E*, CD spectra were recorded in 10 mM sodium phosphate, pH 7.4, 2 mM $MgCl_2$, 1 mM EGTA, 1 mM DTT. *Panel C*, SNAP-25$_{1–90LL}$ (6.8 μM) plus syntaxin$_{1–271}$ (7.1 μM). *Panel D*, SNAP-25$_{1–90GD}$ (8.1 μM) plus syntaxin$_{1–271}$ (7.1 μM). *Panel E*, SNAP-25$_{1–90EE}$ (5.8 μM) plus syntaxin$_{1–271}$ (7.1 μM).

interact electrostatically (24). Coiled coils frequently form the basis of regulated protein-protein interactions, *e.g.* binding and activation of bZIP transcription factors (27, 28).

We have reanalyzed the binding domains of all hitherto reported isoforms of syntaxin and SNAP-25 using two different algorithms (20–22). The results generally confirm the high scores reported earlier. However, there is considerable variation between different species and between the two algorithms, particularly for the NH_2-terminal portion of SNAP-25. In this domain, two sets of heptad repeats were identified (13, see Fig. 8). Although both algorithms yield a probability of 1.0 for coiled coil formation of the second repeat in all species variants, the scores are much more divergent for the first repeat (Lupas (20, 21), using a window size of 27 residues/paircoil (22): rat 1.0/0.68, goldfish 0.99/0.51, *Torpedo* 0.44/0, *Drosophila* 0.36/0, leech 0.02/0). Helical wheel projection of the two putative repeats (Fig. 8, *B* and *C*) shows that according to the predictions Met-40 and Met-43 of the SNAP-25 molecule would be located in the hydrophobic core of a coiled coil. Their replacement with charged side chains would be expected to destabilize a coiled coil interaction, whereas their replacement with appropriate hydrophobic side chains should have little or no effect. These predictions agree with our experimental findings.

Our data show that not only the NH_2-terminal domain of SNAP-25, but also the COOH-terminal domain participates in binding to syntaxin, although, unlike the NH_2-terminal domain, it cannot bind on its own. Binding of the NH_2-terminal domain results in an increase in α-helicity which is similar to but less pronounced than binding of the full-length protein. This difference reflects a true structural difference and not merely a higher relative complex concentration since in 1 M NaCl an increase in α-helicity is only observed when full-length

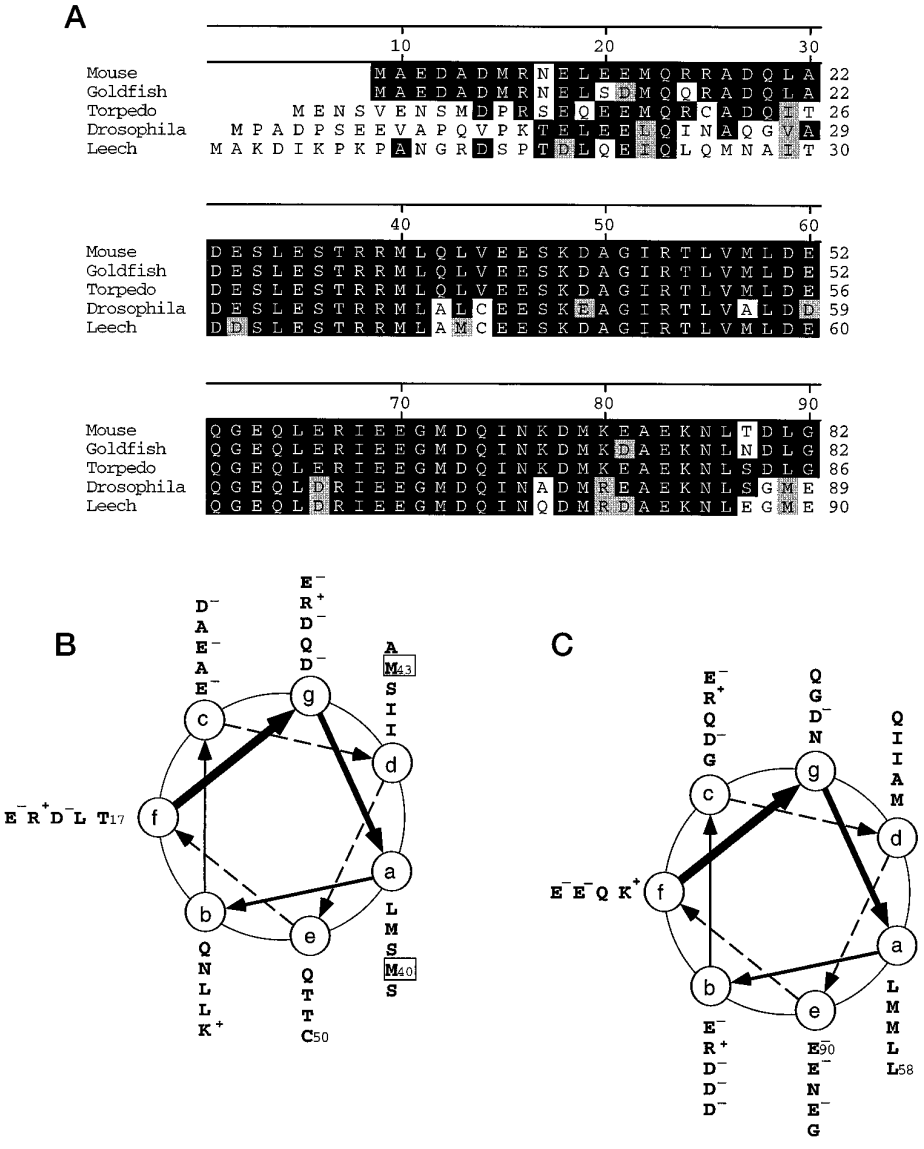

FIG. 8. **The binding region of SNAP-25 to syntaxin contains two putative coiled coil domains.** *Panel A*, sequence alignment of the 1–90 NH_2-terminal fragment of SNAP-25. *Numbering* refers to the leech sequence. Identities are on a *closed black* background. Conservative exchanges of hydrophobic and charged amino acids are on a *gray shaded* background. The mouse sequence is shown as the exon 5b splicing product, which is identical in all tetrapoda SNAP-25 (the GenBank accession number is P13795). The goldfish (*Carassius auratus*) sequence represents the isoform SNAP-25A (P36977). The GenBank accession number for *Torpedo marmorata* is P36976 and for *Drosophila melanogaster*, P36975. *Panels B* and *C*, the sequence of SNAP-25_{1-90wt} is projected onto two helical wheels as predicted by the Lupas (20, 21) and the paircoil (22) algorithm. The first heptad repeat (*panel B*) is predicted to start with Thr-17 in *position f* and to end with Cys-50 in *position e*. The second heptad repeat (*panel C*) starts with Leu-58 in *position a* and ends with Glu-90 in *position e*. The stretch between Gly-51 and Met-57 is not shown. The positions of the introduced point mutations are *boxed*.

SNAP-25 is used. It is likely that the COOH-terminal domain also undergoes a structural change upon binding, although other explanations cannot be ruled out. Previous work has established that the COOH terminus of SNAP-25 is required for binding of synaptobrevin to SNAP-25 (13) and, furthermore, that formation of the SNAP-25-syntaxin complex greatly increases the affinity for synaptobrevin beyond that of either partner alone (9, 11). It is tempting to speculate that formation of the ternary complex is mediated by a global structural change in SNAP-25 which in turn provides an optimized attachment site for synaptobrevin.

Acknowledgments—We thank Luke M. Rice and Isaiah T. Arkin for stimulating discussions and assistance with CD spectroscopy and the coiled coil prediction programs and Phyllis I. Hanson for helpful comments on this manuscript. The λ-Zap library prepared from nerve cord of *H. medicinalis* was kindly provided by Roberta Allen and Steve Heineman of the Salk Institute.

REFERENCES

1. Ferro-Novick, S., and Jahn, R. (1994) *Nature* **370,** 191–193
2. Südhof, T. C. (1995) *Nature* **375,** 645–653
3. Calakos, N., and Scheller, R. H. (1996) *Physiol. Rev.* **76,** 1–29
4. Rothman, J. E., and Wieland, F. T. (1996) *Science* **272,** 227–234
5. Söllner, T., Whiteheart, S. W., Brunner, M., Erdjument-Bromage, H., Geromanos, S., Tempst, P., and Rothman, J. E. (1993) *Nature* **362,** 318–324
6. Söllner, T., Bennett, M. K., Whiteheart, S. W., Scheller, R. H., and Rothman, J. E. (1993) *Cell* **75,** 409–418
7. Hanson, P. I., Otto, H., Barton, N., and Jahn, R. (1995) *J. Biol. Chem.* **270,** 16955–16961
8. Hayashi, T., Yamasaki, S., Nauenburg, S., Binz, T., and Niemann, H. (1995) *EMBO J.* **14,** 2317–2325
9. Hayashi, T., McMahon, H., Yamasaki, S., Binz, T., Hata, Y., Südhof, T. C., and Niemann, H. (1994) *EMBO J.* **13,** 5051–5061
10. Pellegrini, L. L., O'Connor, V., Lottspeich, F., and Betz, H. (1995) *EMBO J.* **14,** 4705–4713
11. Pevsner, J., Hsu, S. C., Braun, J. E., Calakos, N., Ting, A. E., Bennett, M. K., and Scheller, R. H. (1994) *Neuron* **13,** 353–361
12. Calakos, N., Bennett, M. K., Peterson, K. E., and Scheller, R. H. (1994) *Science* **263,** 1146–1149

13. Chapman, E. R., An, S., Barton, N., and Jahn, R. (1994) *J. Biol. Chem.* **269,** 27427–27432
14. Kee, Y., Lin, R. C., Hsu, S. C., and Scheller, R. H. (1995) *Neuron* **14,** 991–998
15. Bruns, D., and Jahn, R. (1995) *Nature* **377,** 62–65
16. Higuchi, R. (1990) in *PCR Protocols: A Guide to Methods and Applications* (Innis, M. A., Gelfand D. H., Sinisky, J. J., White, T. J., eds) pp. 177–183, Academic Press, New York
17. Laemmli, U. K. (1970) *Nature* **227,** 680–685
18. Bradford, M. M. (1976) *Anal. Biochem.* **72,** 248–254
19. Chen, Y. H., Yang, J. T., and Chau, K. H. (1974) *Biochemistry* **13,** 3350–3359
20. Lupas, A., Van Dyke, M., and Stock, J. (1991) *Science* **252,** 1162–1164
21. Lupas, A. (1996) *Methods Enzymol.* **266,** 513–525
22. Berger, B., Wilson, D. B., Wolf, E., Tonchev, T., Milla, M., and Kim, P. S. (1995) *Proc. Natl. Acad. Sci. U. S. A.* **92,** 8259–8263
23. Greenfield, N. J., and Fasman, G. D. (1969) *Biochemistry* **8,** 4108–4116
24. Zhou, N. E., Kay, C. M., and Hodges, R. S. (1994) *J. Mol. Biol.* **237,** 500–512
25. Brennwald, P., Kearns, B., Champion, K., Keranen, S., Bankaitis, V., and Novick, P. (1994) *Cell* **79,** 245–258
26. Crick, F. H. C. (1953) *Acta Crystallogr.* **6,** 689–697
27. Landschulz, W. H., Johnson, P. F., and McKnight, S. L. (1988) *Science* **240,** 1759–1764
28. Weiss, M. A. (1990) *Biochemistry* **29,** 8020–8024